STM JOURNALS

Research & Reviews: Journal of Physics
ISSN: 2278-2265(online), ISSN: 2347-9973(print)
Volume 5, Issue 2
www.stmjournals.com

Evaluation of Image Reconstruction Techniques in Single Photon Emission Computed Tomography (SPECT/CT) Imaging

F. Usman[1,*], R. Zainon[2], A. Saidu[3], A. Bala[3]
[1]School of Physics, Universiti Sains Malaysia, Pulau Penang, Penang, Malaysia
[2]Oncological and Radiological Sciences Cluster, Advanced Medical and Dental Institute, Universiti Sains Malaysia, 13200 Kepala Batas, Pulau Pinang, Malaysia
[3]Department of Physics, Faculty of Science, Usmanu Danfodiyo University Sokoto, Nigeria

Abstract

This work is aimed at evaluating the image reconstruction techniques used in single photon emission computed tomography (SPECT/CT) imaging. The reconstruction techniques considered in this work are: the ordered subset expectation maximization (OSEM) and the Filtered Back Projection (FBP). An anthropomorphic torso phantom with lung and liver inserts was injected with ^{99m}Tc. The liver and the background were given 0.2 MBq/ml and 0.07 MBq/ml respectively. The lungs inserts were filled with polystyrene beads for humanization. A mimicked 30 ml tumor (27 mm) in the liver insert was given 2 MBq/ml sequential SPECT/CT (step and shot, 10 mins over 180° per head) and CT (120 kVp, 80 mAs) projections were acquired using dual head SPECT/16 slice CT system. The projections were reconstructed using OSEM (10 subsets for 2–10 numbers of iterations, Butterworth post filtering, 10 orders and 0.48 frequencies) and FBP (using Butterworth post filtering at 10 order and cutoff frequencies of 0.38–0.58, 0.05 gaps). Image J software was used for the image analysis. Statistical t-test tested the mean gray values of the tumor and its background. The OSEM and FBP reconstructed images were evaluated from their contrast-to-noise ratio (CNR). The optimal parameter was selected based on 3–5 CNR detection range set by the Rose criterion. The t-test showed the background and the tumors mean values to be statistically significant ($P \ll 0.05$). The CNR values for FBP images were all below the detection range, maximum value at the cutoff frequency 0.48 (1.69). In OSEM images at cutoff frequency 0.48, the CNR values were within the detection range for 2–8 numbers of iteration with maximum value (4.89) at 4 numbers of iteration. OSEM was found to be the best for tumor detection and administered activity can be reduced at 4 OSEM's of iterations (40 MLEM iterations) for patient safety.

Keywords: *Anthropomorphic torso phantom, ^{99m}Tc, SPECT, iterative reconstruction, CNR, P-Value, liver*

****Author for corresponding*** E-mail: fahatu11@gmail.com

INTRODUCTION

Malignant liver tumors (both the primary and the metastatic ones) can be treated with conventional radiation treatment procedures [1]. But a more promising catheter based treatment procedure; radioembolisation using yttrium-90 (^{90}Y) microspheres has shown to be the best [2]. This is due its lower toxicity among the others [3]. Although, using the spheres has the potential of treating the abnormalities, improper targeting of the yttrium-90 (^{90}Y) microspheres to tumors in the liver, may lead to many diseases collectively known as radioembolisation induced liver disease (REILD) [3–5]. In order to avoid this problem, nuclear medicine imaging using ^{99m}Tc-MAA has been used as a pre-therapeutic agent. This is resulted from its help in the evaluation of extrahepatic abdominal shunting as well as in the evaluation of intrahepatic tracer distribution [3]. The distribution of the tracer, which the imaging outlines, shows the extent of the tumor in the liver. This makes the spheres to be localised in the appropriate position [6–9].

Initially, planer imaging was the only nuclear medicine imaging technique employed in

imaging liver and other body organs or structures using nuclear medicine procedures [10–13]. The emergent of single photon emission computed tomography (SPECT/CT) overshadowed the planer imaging due to its prominent feature of overcoming the structure overlapping property associated with planer imaging [13–15]. Many studies shows the efficiency of SPECT/CT in increasing sensitivity, specificity and detectability compared to planer image [11, 12, 16–20]. Moreover, due to inheriting low counts associated with nuclear medicine imaging it generally suffer from serious problem of poor resolution and high amount of noise [1, 10, 21–24]. The use high radiation doses are also avoided in nuclear imaging, because the substance will stay within the body and circulate through the entire body. Thus, SPECT/CT being part of nuclear medicine is not an exception. Furthermore, the problem of attenuation and scattering of the photons has shown to displace the imaged abnormality from its correct location. Many studies have shown the utilization of an appropriate reconstruction techniques (capable of modelling the physical processes involved in the formation of the image) in tackling the problems [25–27]. Furthermore, other problems come into being; the fact that SPECT/CT imaging shows only functional processes of the subject or volume of interest. Therefore, it lacks the anatomical information, which makes the proper delineation of tumors difficult or impossible in some case.

The fusing of the SPECT/CT image with another image containing high contrast anatomical information from different modality (like computed tomography (CT) or magnetic resonance imaging) has shown to improved diagnosis by complementing the required information [10, 12, 28–30]. This fusion of the image developed from the conventional software fusing to current hardware fusing. The later is possible with current hybrid SPECT/CT systems available in most of the current nuclear medicine centers. Its main important feature is SPECT fusion with CT acquired from the same patient bed. This is contrary to the software fusing, which involve images acquired at different time and different patient arrangement. Many studies show an improvement in diagnosis through the use of hardware fusion capability of hybrid SPECT/CT systems [28–35]. The presence CT also helps in providing the attenuation map, which is utilized in making attenuation corrections [30, 36, 37].

The proper selection of acquisition parameters, reconstruction techniques and reconstruction parameters are among the most essential factors that complements the attainment of an optimal quality SPECT/CT images. By selecting proper mode of SPECT image acquisition and certain selection of CT acquisition parameters, the SPECT/CT image of certain quality can be obtained [11, 27, 38–42]. For example, studies on acquisition modes in SPECT show that both the continuous and the step and shoot modes have their own advantages and disadvantages. The former due to its characteristic of having its camera head rotating continuously, it tends to be more sensitive compared with the former. This is because counts are being recorded continuously as it rotates. However, the former is having a relatively higher resolution due to the slow movement of the camera head during the type of the acquisition. Therefore, it acquires counts statically and moves to the next step. This makes exploiting these opposing properties useful in the attainment of a good standard acquisition protocol, a tradeoff between an optimal sensitivity and an optimal resolution. Furthermore, regarding the issue of reconstruction techniques and selection of their parameters', many qualitative image quality evaluation methods and few quantitative ones were conducted. Among the two common reconstruction techniques (OSEM and FBP), OSEM has shown to be the most preferred in terms of providing an optimal information (particularly improved contrast-to-noise ratio, CNR) [14, 15, 27, 43].

In addition, the noise level increases with increased number of iterations (leading to reduced CNR value). Furthermore, OSEM is capable of making resolution recovery corrections, scattered corrections and attenuation corrections. However, its disadvantages are; having relatively (to FBP) slow convergence (this means that lower numbers of iterations are poor related to real image), amplification of noise with increasing number of iterations, and the dependence of its

characteristics on source distribution [43]. FBP on the other hand is characterized by relatively high noise level and better spatial resolution (hence, most prepared quantitatively, because of its greater convergence) [44]. The characteristics of these two reconstruction algorithms created a lot of confusions on the optimum parameter selection for quantitative measurement from the algorithms. Also, selecting appropriate parameters depends on the purpose of the imaging as well as the type of the lesions [11]. It is commonly and well known that qualitative method of evaluation is the preferred method used in the clinical settings [11, 12, 28, 30]. But it aches from a great detection problem due to subjective nature. In which accurate evaluation or diagnosis depends on the experience of the radiologist, how healthy is the radiologist's vision among the others. This makes a great deal of false positive or improper diagnosis [11].

In order to do away with all these problems, this work focuses on liver tumor for the evaluation of the optimal reconstruction algorithms and their parameters using quantitative evaluation method. Particularly, the evaluation of the most essential image quality determiner called contrast-to-noise ratio. This parameter is defined by the use of Rose criterion. This states that optimum detection requires a signal's magnitude at least three times that of the noise [11]. This condition of the Rose criterion would be of great help in determining whether the parameter's value allows lesion's detection or not. Ultimately, it would enable proposing an optimum reconstruction algorithm and its parameter's selection within detectability range.

The result would be benefited by the nuclear medicine technologists in the acquisition of the liver SPECT/CT image. However, it would reduce the incorrect interpretations of the SPECT/CT image especially among the less experience interpreters. Therefore, proper management of liver abnormalities (and may also be applicable to SPECT/CT imaging of other structures) and at the same time minimizing dose to the patients would be attained.

MATERIALS AND METHODS

Subject and Data Acquisition Area

The data acquisition was held at the Nuclear Medicine unit, Clinical trial Center, Advanced Medical and Dental Institute, Universiti Sains Malaysia. The unit has installed dual camera 16 slice hybrid SPECT/CT system (Figure 1), which was utilized for the image acquisition. The anthropomorphic torso phantom (Figure 2) with background volume of 10.3 liters contains liver insert (volume 1.2 liters), lung insert (0.9 liters and 1.1 liters for left and right respectively) and optional cardiac insert. The acquisition of the SPECT/CT image was conducted with the cardiac insert not in place. The work focused on liver insert of the phantom. In the liver insert, a tumor was mimicked using a syringe sphere of about 27 mm diameter, volume of about 30 ml. The diameter of such magnitude was chosen so as prevent partial volume effect by allowing it to exceed the system's spatial resolution, which is about 13 mm FWHM.

Fig. 1: *SPECT/CT System.*

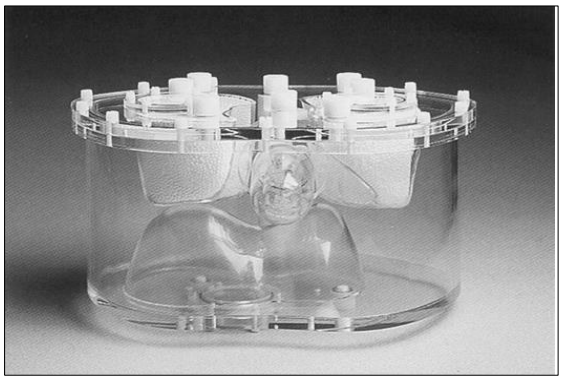

Fig. 2: *Anthropomorphic Torso phantom.*

SPECT Acquisition and its Parameters

Two different SPECT/CT acquisitions were performed for 12 minutes each, using step and shoot acquisition mode and continuous acquisition mode following injecting the phantom with ^{99m}Tc, the radioactivity concentrations injected were 0.07 MBq/ml, 0.2 MBq/ml and 2 MBq/ml for the background, liver insert of the phantom and the sphere respectively. Data were acquired using the dual-detector (adjustable) multi-slice (16 slice) CT Scanner (General Electric) equipped with low-energy high-resolution parallel-hole collimators (LEHR). Data were acquired as 128 × 128 matrices for 120 projections (60 per gamma camera head) at 10 seconds/projection using the 'step and shoot mode'. The tomographic projection views were acquired over an arc of 360°. Energy discrimination was accomplished with a 20% energy window centered on 140 keV. The CT component of the examination was acquired immediately after the SPECT component, without changing the phantom arrangement position. The CT was acquired using a diagnostic setting of 120 kVp at 80 mA and 0.8 s. Furthermore, the unit was set to acquire 3.75 mm thick slices in spiral acquisition mode. This made the data obtained from the CT acquisition perfect for 3D imaging (because of the lack of motion mis-registration) and the increased out of plane resolution (due fastest nature associated with it relative to the conventional method of acquisition). The CT data were acquired into 256 × 256 matrices. The CT scan was conducted in 2 minutes; which makes the total acquisition time for the SPECT/CT, 12 minutes as mentioned.

SPECT Image Reconstruction Techniques

The SPECT projections data acquired from the 'step and shoot' acquisition mode were sent to the processing unit of the department, where image processing personal computers (PCs) were situated. The processing PCs were installed with Xyleris software containing FBP and OSEM reconstruction capabilities. The data were reconstructed by both the FBP and OSEM reconstruction algorithms, using different parameters selection. For OSEM reconstruction algorithm, the projection data was reconstructed using 10 numbers of subsets, with 2, 3, 4, 5, 6, 7, 8, 9, and 10 numbers of iterations. The post-filtration was made using a Butterworth filter, cutoff frequency 0.48 and order 10 for all the OSEM reconstructed images. Also for the FBP reconstruction, Butterworth filter was used for the noise suppression with fixed order of 10 and cutoff frequencies of 0.38, 0.43, 0.48, 0.53 and 0.58 were used in reconstructing the projection data. Following the CT reconstruction, the two images of the different modalities were fused (registered). Furthermore, the OSEM algorithm incorporated corrections for collimator-specific resolution recovery corrections, scattering corrections, and CT-attenuation corrections.

Statistical Analysis of SPECT Using Image J Software and Statistical Test

The analysis of the SPECT/CT was conducted using an open source image processing software called Image J. It is a software base on java, which was developed at the National Institute of Health, Bethesda, Maryland, USA. Because of its open nature, accessibility to it became easy. However, image processing PCs gives the reconstructed SPECT images' information in DICOM format. This prevented it from losing any of its property.

The t-test (also sometimes called the Student t-test) was then used to determine the significance of the difference between the means of the background and tumor. This test was aimed at comparing the difference in means relative to the observed random variations in tumor and the background. The significance level of 0.05 levels was set, therefore for all the tests, probability (p) values < 0.05 were considered statistically significant and the null hypothesis was rejected. The statistical test was conducted Microsoft excel 2007 version, using Independent data and one-sided test selection (one tail distribution). All the data were ensured statistically significant before the image quality evaluation was commenced.

Evaluation of Image Quality in SPECT and its Parameters

Following the statistical calculations and the statistical tests, SPECT/CT image quality was evaluated. Because of the tomographic reconstruction process in SPECT/CT image, its noise is no longer Poissonian, it does not

have a uniform (white) power spectrum and it depends on a number of parameters: counts acquired, the distribution of the counts, the reconstruction process among the others. Consequently, the raw signal-to-noise ratio is not well behaved and therefore, we used a measure of tomographic contrast, or tomographic contrast-to-noise ratio, in assessing the detection ability of the SPECT/CT image. It was calculated using the following formulas. However, the two components of the formula, contrast and coefficient of variation (which describes the noise) were evaluated first.

Contrast

This refers to the differences in density (or intensity) in parts of the image. It was evaluated using the following relation.

Contrast $C = \frac{\overline{S} - \bar{b}}{\bar{b}}$ [11]

Where, $\overline{S}$ is the mean value of the high concentration VOI (tumor) and $\bar{b}$ is the mean value of the background VOI.

Noise (Represented by the Background Standard Deviation)

This can be described as an undesirable by-product of image capture that adds spurious and extraneous information. Statistical noise can impair detectability, especially if the object has low contrast. The coefficient of variation (N), also known as "relative variability", which was used in calculating the CNR, equals the standard deviation divided by the mean. It was expressed as a fraction.

$$\boldsymbol{N = \frac{\sigma b}{\bar{b}}} \quad \textbf{[11]}$$

Following the components' evaluation, the essential parameter for evaluating detection ability, the CNR of the object in the image was then evaluated. Conclusion was reached that, for detection ability to be achieved, an object's CNR must exceed 3–5 [11]. This condition is known as the Rose criterion.

Contrast-to-Noise Ratio $(CNR) = \frac{C}{N}$ [11]

Where, N is the noise contrast (coefficient of variation), $\boldsymbol{\sigma_b}$ is the standard deviation of the background, $\bar{\mathbf{b}}$ is the mean intensity of the background counts, $\overline{S}$ is the mean value of the high concentration VOI (tumor) and C is its contrast.

RESULTS

Statistical Test

The statistical t-test was conducted using Microsoft excel, 2007 version. It showed the uptake between the liver background and simulated tumor to be statistically significant. The values obtained were 2.11053E-17 and 2.41436E-06 for the OSEM reconstructed SPECT/CT (step and shoot acquisition) using 10 subsets and FBP reconstructed images (step and shoot acquisition). Therefore, the p-value threshold for the significant test (p-values < 0.05), proves the above result to be statistical significant. Ultimately, the quantitative analysis using the data became authorized.

Liver SPECT/CT Image Quality Evaluation (Assessing Detectability of the Tumor)

The CNR (as the parameter that determine the limit of lesion detection) of the SPECT/CT image was evaluated for varieties of parameters of the FBP and OSEM reconstruction algorithms. The result showed a very interesting pattern. The FBP reconstructed SPECT/CT image for different cutoff frequencies gave different value of the CNR value. The value was raised at the center of the curve. Specifically, it occurred at a point that corresponds to the cutoff frequency of 0.48 and order of 10. However, the value diminished again in a pattern similar to the initial take up pattern of the curve (Figure 3). Although, the CNR value showed the raising pattern at 0.48 cutoff frequency, but the value obtained (1.69) is below the Rose criterion limit set for the detection (Table 1). OSEM reconstructed images on the other hand, showed a CNR value at 0.48 cutoff frequency within the detection ability range defined by the Rose criterion (Table 2). However, the CNR value changed with changing numbers of iterations (Figure 2). Furthermore, the pattern of the graph (Figure 4) was similar to that obtained for the FBP. But, in this case the CNR variation depends on numbers of iterations as opposed FBP graph (Figure 3) which was depended on variation in cutoff frequencies. The OSEM graph gave a CNR result that reached its maximum value at about 4 numbers of iterations. In addition, all the other numbers of iterations gave CNR value that fell within the detection ability range with the exception of 9 and 10 numbers of iterations.

Table 1: *CNR for FBP reconstructed SPECT/CT (step and shoot acquisition) Using 10 Subsets versus Cutoff Frequencies.*

Cut off frequency	CNR
0.38	1.39
0.43	1.42
0.48	1.69
0.53	1.37
0.58	1.36

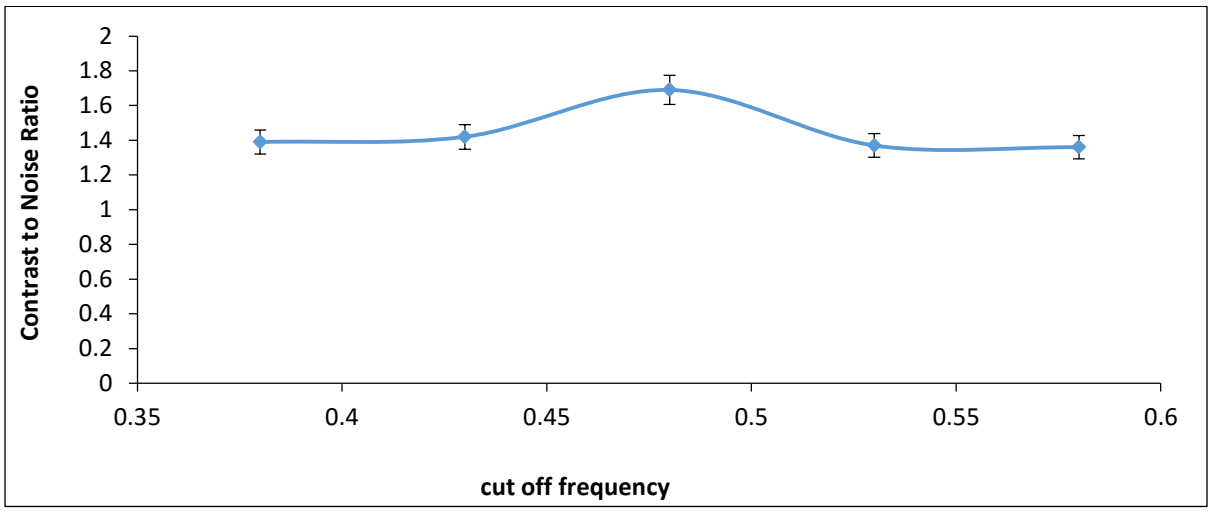

Fig. 3: *CNR for FBP Reconstructed SPECT/CT (step and shoot acquisition) Using 10 Subsets Versus Cutoff Frequencies.*

Table 2: *CNR for OSEM reconstructed SPECT/CT (step and shoot acquisition), 10 Subsets versus Numbers of Iterations.*

iterations	CNR
2	3.71
3	3.84
4	3.89
5	3.67
6	3.58
7	3.38
8	3.17
9	2.57
10	2.01

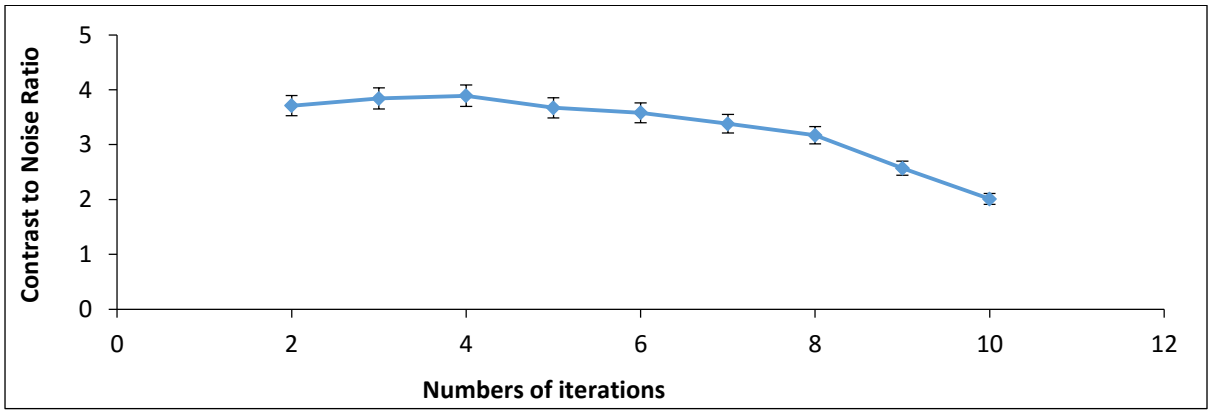

Fig. 4: *CNR for OSEM Reconstructed SPECT/CT (step and shoot acquisition), 10 Subsets versus Numbers of Iterations.*

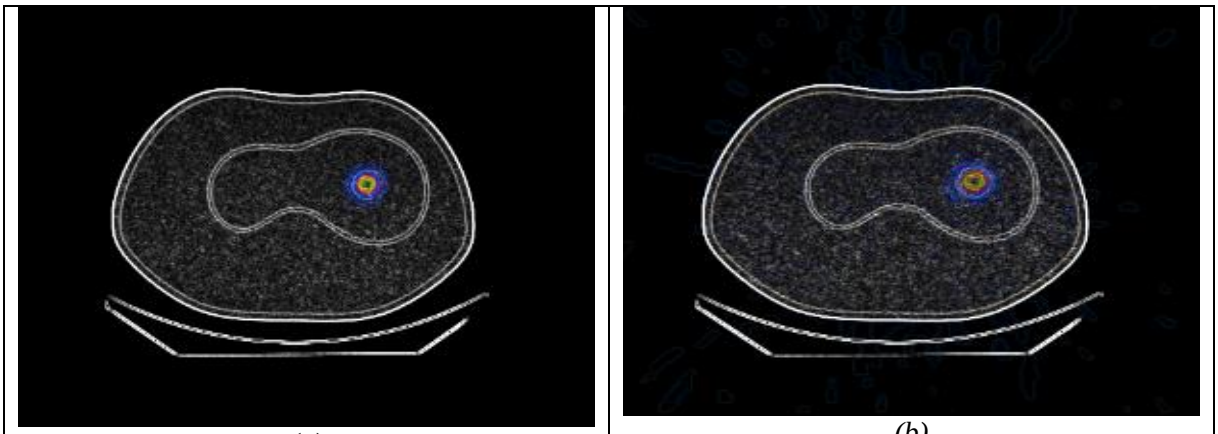

(a) *(b)*

Fig. 5: *(a) Sample of OSEM Reconstructed Liver SPECT/CT Image at 2 Iterations and 10 Numbers of subset. (b) Sample of FBP Reconstructed Liver SPECT/CT Image at O.38 Cutoff Frequency and 10 Orders.*

DISCUSSION

Many researchers have found the utilization of SPECT/CT imaging to be superior to both the planer and the SPECT alone images in terms of image quality [9, 12, 28, 35]. In addition, [43, 39] and [32] studied the choice of proper reconstruction algorithms. According to them, the choice plays an important role toward achieving optimal quality image. Furthermore, studies revealed that, the effects of the reconstruction parameters on SPECT/CT image quality depend on the purpose (objective) of the investigation and the nature of the subject (region of interest) [10, 11, 45]. Thus, any alteration in the parameters is expected to affect the SPECT/CT image quality (Figure 5).

The OSEM'S CNR Value obtained from this work is in consistence with many studies on reconstruction techniques evaluation [30, 31, 43, 46]. In broad sense, the CNR values from Figure 1 (FBP reconstructed images) were shown to increase with increase in the cutoff frequency. This is resulted from the blockage of the high frequency noise by the Butterworth filter. Initially, at 0.38, the high frequency suppression resulted in over smoothening of the SPECT/CT image. Consequently, the contrast is degraded and as such the SPECT/CT CNR value is low. However, as the cutoff frequency is increased to 0.43, the contrast is relatively less degraded. This made the CNR value to increase a little bit. The better tradeoff (peak CNR value) between the noise level and the contrast was reached at 0.48. After then, the increase in the cutoff frequency made the increase in noise significant over the contrast. This made the CNR value to be degraded at 0.53 and 0.58. This pattern is expected to be maintained henceforth. This is resulted from the possible increase in noise build up with greater numbers of iterations. In other words, as we increase the iterations, the inherent noisy liver SPECT/CT image is approaching its reality. Regarding the OSEM reconstructed images; the 0.48 cutoff frequency was adopted from the result obtained in FBP reconstruction. Although, it is accepted that any increase in the numbers of iterations attracts amplification of high frequency noise. The result obtained in this study gave an alternating and interesting result. In our work, the fixed cutoff frequency of 0.48 made constant noise suppression. However, the CNR values of the SPECT/CT image were increase from 2 numbers of iteration to highest CNR value at 4 numbers of iterations. Furthermore, the CNR maintained a degrading pattern after the peak. This is better explained from the aforementioned character in achieving convergence. In an elaborating perspective however, the increase in the CNR with increasing numbers of iterations depicted the significance of contrast over noise. On the other hand, the CNR values after the peak (4 numbers of iterations) depicted the significance of noise over contrast. In addition, the values of CNR below the detection range in FBP reconstructed SPECT/CT images are attracting. This better described the inability of the reconstruction algorithm to correct for

degrading factors like scattering, attenuation and collimator detector response. Consequently, for detection purpose in liver SPECT/CT imaging OSEM algorithm should be the best. As highlighted, this is backed by many studies on the issue. However, the uniqueness in the liver SPECT/CT image calls for an optimal CNR value at 4 numbers of iterations. In addition, this may be interpreted to play a role in managing patient radiation absorbed dose. Consequently, the dose can be minimized by reducing the activity of the radiopharmaceuticals at the peak points. The reduction can still yield CNR value that could be within the detection limit.

CONCLUSION

OSEM is the best for liver tumor detection. In addition, administered activity can be reduced at 4 OSEM's of iterations (40 MLEM iterations) for patient safety in terms of exposure to radiation. This can also be extended to personnel safety as well.

REFERENCES

1. Abdallah YMY, E Wagiallah. Enhancement of Nuclear Medicine Images using Filtering Technique. System. 2014; 5: 6p.
2. Salem R et al. Radioembolization for hepatocellular carcinoma using Yttrium-90 microspheres: a comprehensive report of long-term outcomes. Gastroenterology. 2010. 138(1): 52–64p.
3. Ahmadzadehfar H, H-J Biersack. Clinical applications of SPECT-CT. 2013: Springer Science & Business Media.
4. Sangro B, M Iñarrairaegui, A.S. Kennedy. Radioembolization-Induced Liver Disease, in Liver Radioembolization with 90Y Microspheres. 2013, Springer. p. 177–185.
5. Hickey R, R Lewandowski, R Salem. Yttrium-90 radioembolization is a viable treatment option for unresectable, chemorefractory colorectal cancer liver metastases: further evidence in support of a new treatment paradigm. Annals of Surgical Oncology. 2015. 22(3): p. 706–707.
6. Gates VL et al. Intraarterial Hepatic SPECT/CT Imaging Using 99mTc-Macroaggregated Albumin in Preparation for Radioembolization. Journal of Nuclear Medicine. 2015. 56(8): p. 1157–1162.
7. Shah K et al. 99m Technetium-Macroaggregated Albumin (MAA) SPECT/CT Liver Perfusion Imaging Prior to Radioembolization: Patterns and Pitfalls of Extrahepatic Activity. Journal of Nuclear Medicine. 2015; 56(Supplement 3): 1876–1876p.
8. Ahmadzadehfar H, et al. The role of SPECT/CT in radioembolization of liver tumours. European Journal of Nuclear Medicine and Molecular Imaging. 2014; 41(1): 115–124p.
9. Walrand S. Bremsstrahlung SPECT/CT, in Clinical Applications of SPECT-CT. 2014, Springer. p. 271–280.
10. Glaudemans AWJM, A. Signore. Nuclear Medicine Imaging Modalities: Bone Scintigraphy, PET-CT, SPECT-CT, in Bone Metastases. 2014, Springer. p. 71–94.
11. Cherry SR, JA Sorenson, ME Phelps. Physics in nuclear medicine. 2012: Elsevier Health Sciences.
12. Lavely WC, et al. Comparison of SPECT/CT, SPECT, and planar imaging with single-and dual-phase 99mTc-sestamibi parathyroid scintigraphy. Journal of Nuclear Medicine. 2007; 48(7): 1084–1089p.
13. Madsen MT. Recent advances in SPECT imaging. Journal of Nuclear Medicine. 2007; 48(4): 661–673p.
14. Mettler Jr FA, MJ Guiberteau. Essentials of nuclear medicine imaging. 2011: Elsevier Health Sciences.
15. Powsner RA, ER Powsner. Essential nuclear medicine physics. 2008: John Wiley & Sons.
16. Ritt P, et al. Absolute quantification in SPECT. European Journal of nuclear Medicine and Molecular Imaging. 2011; 38(1): 69–77p.
17. Groch MW, WD Erwin. SPECT in the year 2000: basic principles. Journal of Nuclear Medicine Technology. 2000; 28(4): 233–244.
18. Ahmadzadehfar H, M Hoffmann. Therapy Planning with SPECT/CT in Radioembolisation of Liver Tumours, in Clinical Applications of SPECT-CT. 2014, Springer. p. 255–270.
19. Shen S, et al. A technique using 99m Tc-mebrofenin SPECT for radiotherapy treatment planning for liver cancers or

metastases. Medical Dosimetry. 2014; 39(1): 7–11p.
20. Lukovic J, B Yaremko, RR Reid. Functional Lung Avoidance Using Ventilation SPECT in the Treatment of Advanced-Stage Carcinoma of the Lung: A Treatment Planning and Feasibility Study. International Journal of Radiation Oncology Biology Physics. 2014; 90(1): S212p.
21. Ott RJ, R Stephenson. Electronics Related to Nuclear Medicine Imaging Devices. Chapter 7, in Nuclear Medicine Physics: A Handbook for Teachers and Students. Endorsed by: American Association of Physicists in Medicine (AAPM), Asia–Oceania Federation of Organizations for Medical Physics (AFOMP), Australasian College of Physical Scientists and Engineers in Medicine (ACPSEM), European Federation of Organisations for Medical Physics (EFOMP), Federation of African Medical Physics Organisations (FAMPO), World Federation of Nuclear Medicine and Biology (WFNMB). 2014.
22. Fahey FH, R Lim, G El-Fakhri. Physical Aspects of Pediatric Nuclear Medicine Imaging, in Pediatric Nuclear Medicine and Molecular Imaging. 2014, Springer. p. 621–643.
23. Lewellen TK, et al. A Building Block for Nuclear Medicine Imaging Systems Data Acquisition. Nuclear Science. IEEE Transactions on, 2014. 61(1): p. 79–87.
24. Treves ST, AE Falone, FH Fahey. Pediatric nuclear medicine and radiation dose. Elsevier.
25. Yoneyama H, et al. Optimization of attenuation and scatter corrections in sentinel lymph node scintigraphy using SPECT/CT systems. Annals of Nuclear Medicine. 2015; 29(3): 248–255p.
26. Livieratos L. Technical Pitfalls and Limitations of SPECT/CT. Elsevier.
27. Okuda K, et al. Optimization of iterative reconstruction parameters with attenuation correction, scatter correction and resolution recovery in myocardial perfusion SPECT/CT. Annals of Nuclear Medicine. 2014; 28(1): 60–68p.
28. Mariani G, et al. A review on the clinical uses of SPECT/CT. European Journal of Nuclear Medicine and Molecular Imaging. 2010; 37(10): 1959–1985p.
29. Kaufmann PA, MF Di Carli. Hybrid SPECT/CT and PET/CT imaging: the next step in noninvasive cardiac imaging. Elsevier.
30. Kim EE. Clinical Applications of SPECT-CT. Journal of Nuclear Medicine. 2014; 55(12): 2078–2078p
31. Bailey DL, KP Willowson. Physics and Technology of SPECT/CT, in Clinical Applications of SPECT-CT. 2014, Springer. p. 1-27.
32. Buck AK, et al. Spect/Ct. Journal of Nuclear Medicine. 2008; 49(8): 1305–1319p.
33. Bybel B, et al. SPECT/CT Imaging: Clinical Utility of an Emerging Technology 1. Radiographics. 2008; 28(4): 1097–1113p.
34. Mansi L, V Cuccurullo, PF Rambaldi. SPECT-CT: Importance for clinical practice, in Atlas of SPECT-CT. 2011, Springer. p. 1–8.
35. Leitha T, A Staudenherz. Hybrid PET/CT and SPECT/CT imaging. Computed tomography-clinical applications. InTech. 2012.
36. Bernstine H, et al. Comparison of 80 and 120 kVp contrast-enhanced CT for attenuation correction in PET/CT, using quantitative analysis and reporter assessment of PET image quality. Clinical Radiology. 2014; 69(1): e17-e24p.
37. Izquierdo-Garcia D, et al. Comparison of MR-based attenuation correction and CT-based attenuation correction of whole-body PET/MR imaging. European Journal of Nuclear Medicine and Molecular Imaging. 2014; 41(8): 1574–1584p.
38. Bruyant PP. Analytic and iterative reconstruction algorithms in SPECT. Journal of Nuclear Medicine. 2002; 43(10): 1343–1358p.
39. Knoll P, et al. Comparison of advanced iterative reconstruction methods for SPECT/CT. Zeitschrift für medizinische Physik. 2012; 22(1): 58–69p.
40. Koch W, et al. Is iterative reconstruction an alternative to filtered backprojection in routine processing of dopamine transporter SPECT studies? Journal of Nuclear Medicine. 2005; 46(11): 1804–1811p.

41. Koral KF, et al. Optimizing the number of equivalent iterations of 3D OSEM in SPECT reconstruction of I-131 focal activities. Nuclear Instruments and Methods in Physics Research Section A: Accelerators, Spectrometers, Detectors and Associated Equipment. 2007. 579(1): 326–329p.
42. McConnell D, et al. Evaluation of an iterative reconstruction algorithm that models the detector response of the PET scanner. Journal of Nuclear Medicine. 2012; 53(Supplement 1): 2618–2618p.
43. Nichols KJ, GG Tronco, CJ Palestro. Effect of reconstruction algorithms on the accuracy of 99mTc sestamibi SPECT/CT parathyroid imaging. American Journal of Nuclear Medicine and Molecular Imaging. 2015; 5(2): 195p.
44. Ziegler A, T Köhler, R Proksa. Noise and resolution in images reconstructed with FBP and OSC algorithms for CT. Medical Physics. 2007; 34(2): 585–598p.
45. Keidar Z, O Israel, Y Krausz. SPECT/CT in tumor imaging: technical aspects and clinical applications. Elsevier.
46. Erdogan H, JA Fessler. Ordered subsets algorithms for transmission tomography. Physics in Medicine and Biology. 1999; 44(11): 2835p.

Cite this Article

F. Usman, R. Zainon, A. Saidu, A. Bala. Evaluation of image reconstruction techniques in Single photon emission computed tomography (SPECT/CT) imaging. *Research & Reviews: Journal of Physics.* 2016; 5(2): 13–22p.